Supporting Information for Stresses in the lunar interior: insights from slip directions in the A01 deep moonquake nest

A. R. Turner [1], J.C. Hawthorne [1] and M. Gaddes [2]
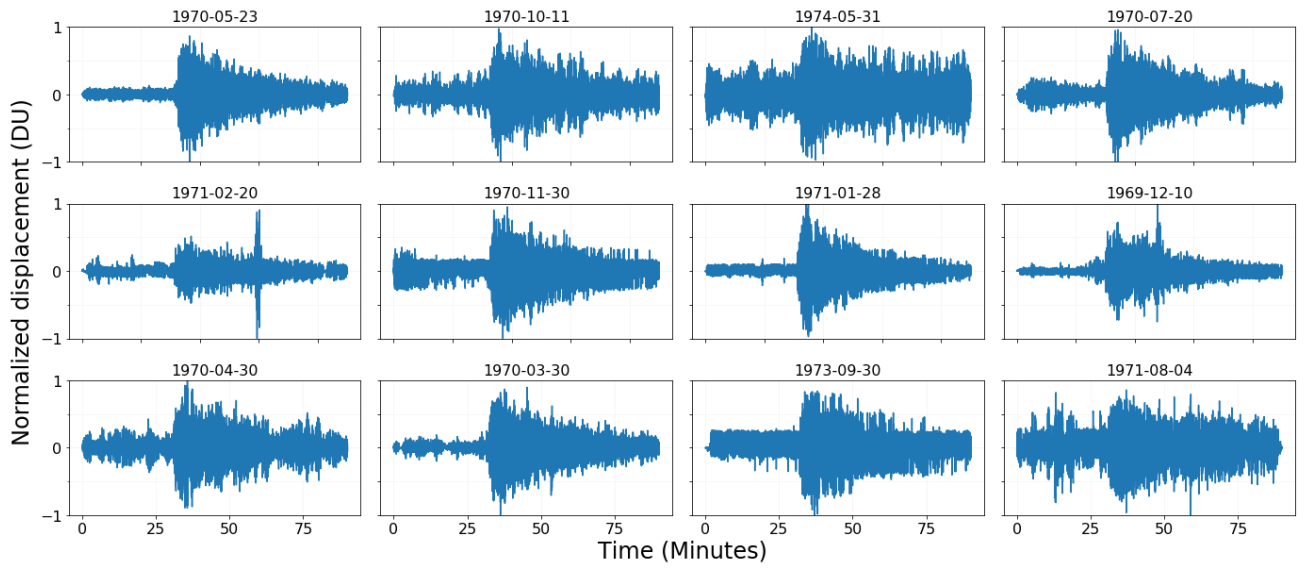
[1]Department of Earth Sciences, University of Oxford, Oxford, UK
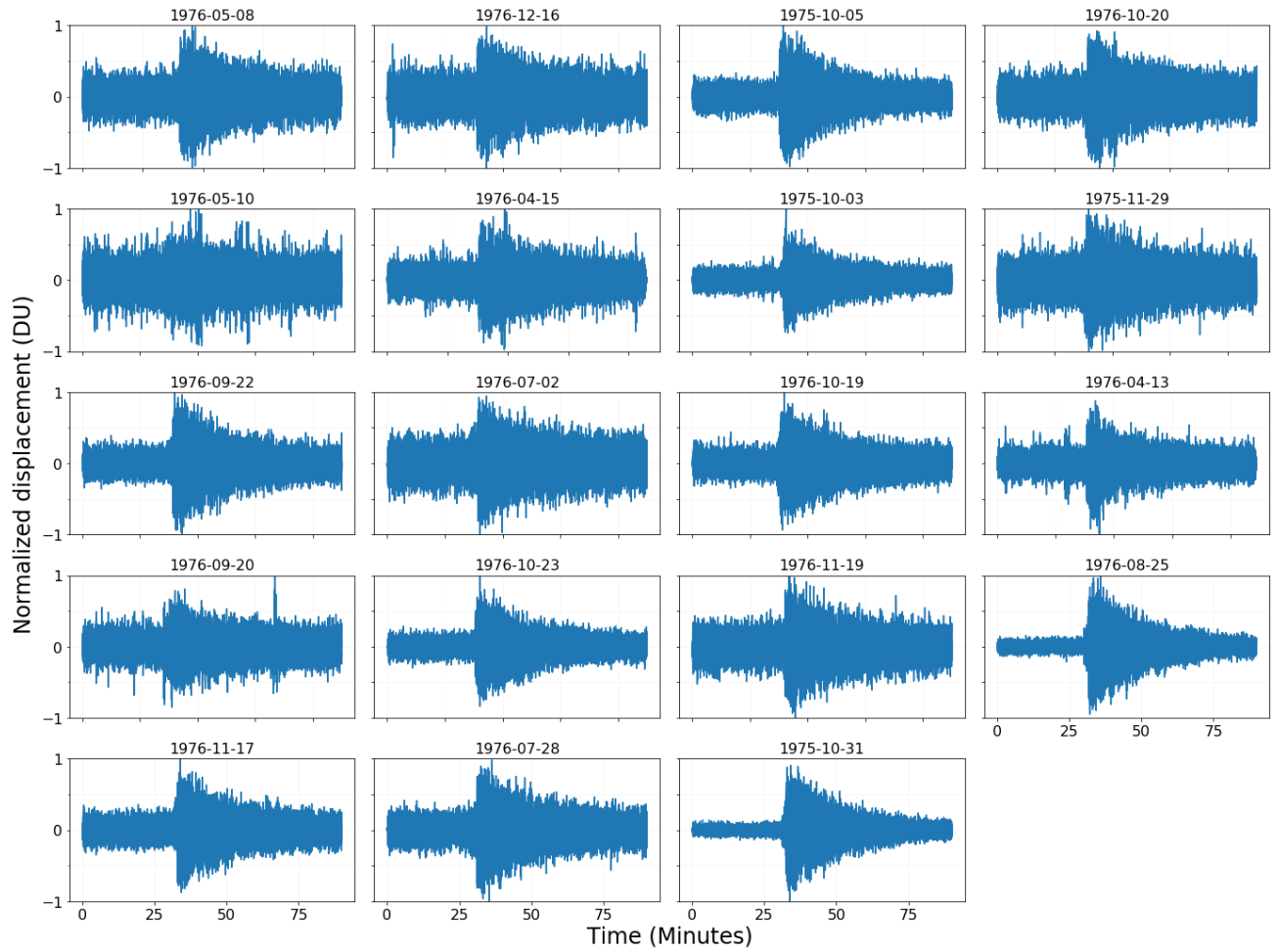
[2]COMET, University of Leeds, Leeds, UK
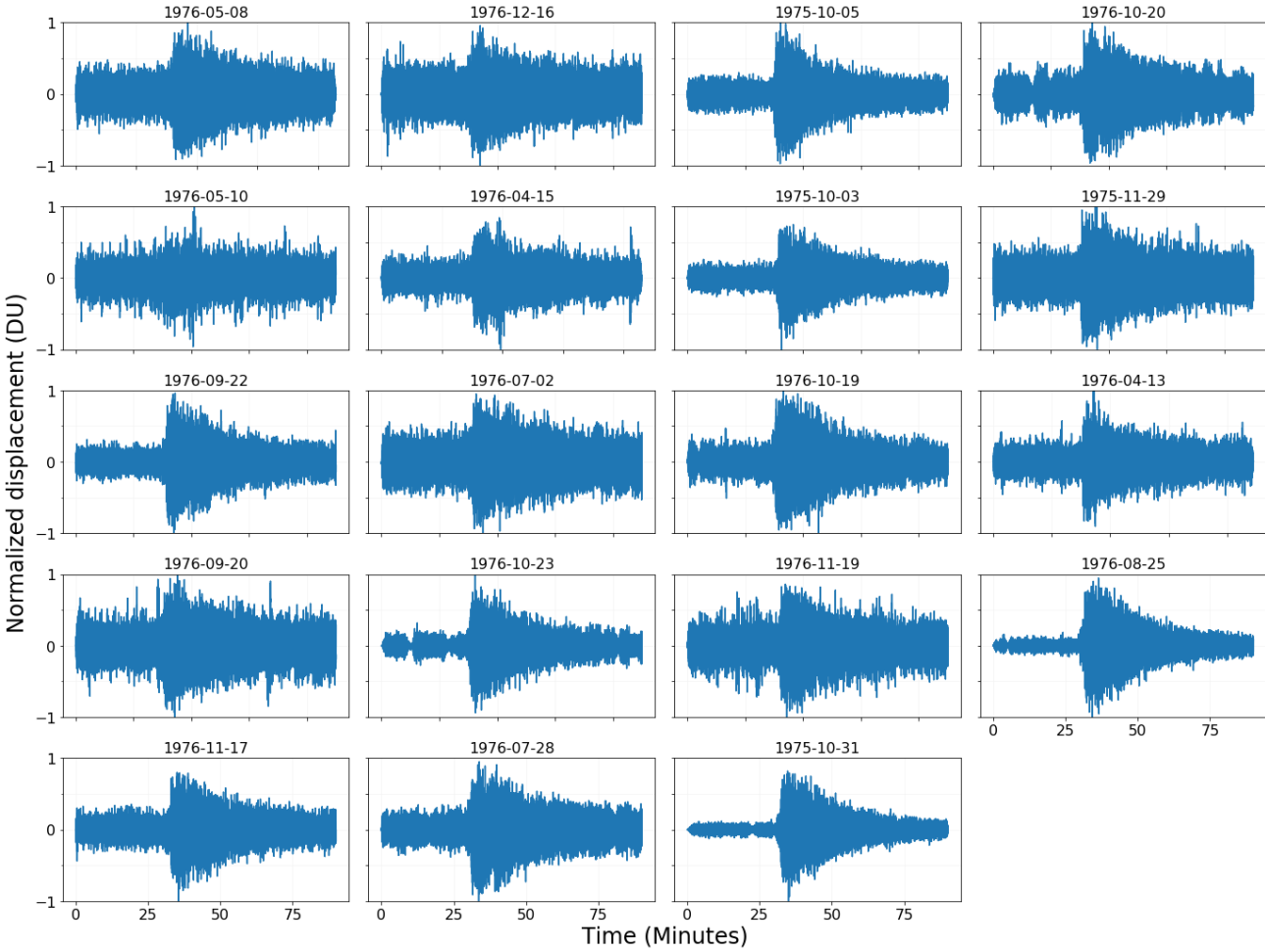
Contents of this file
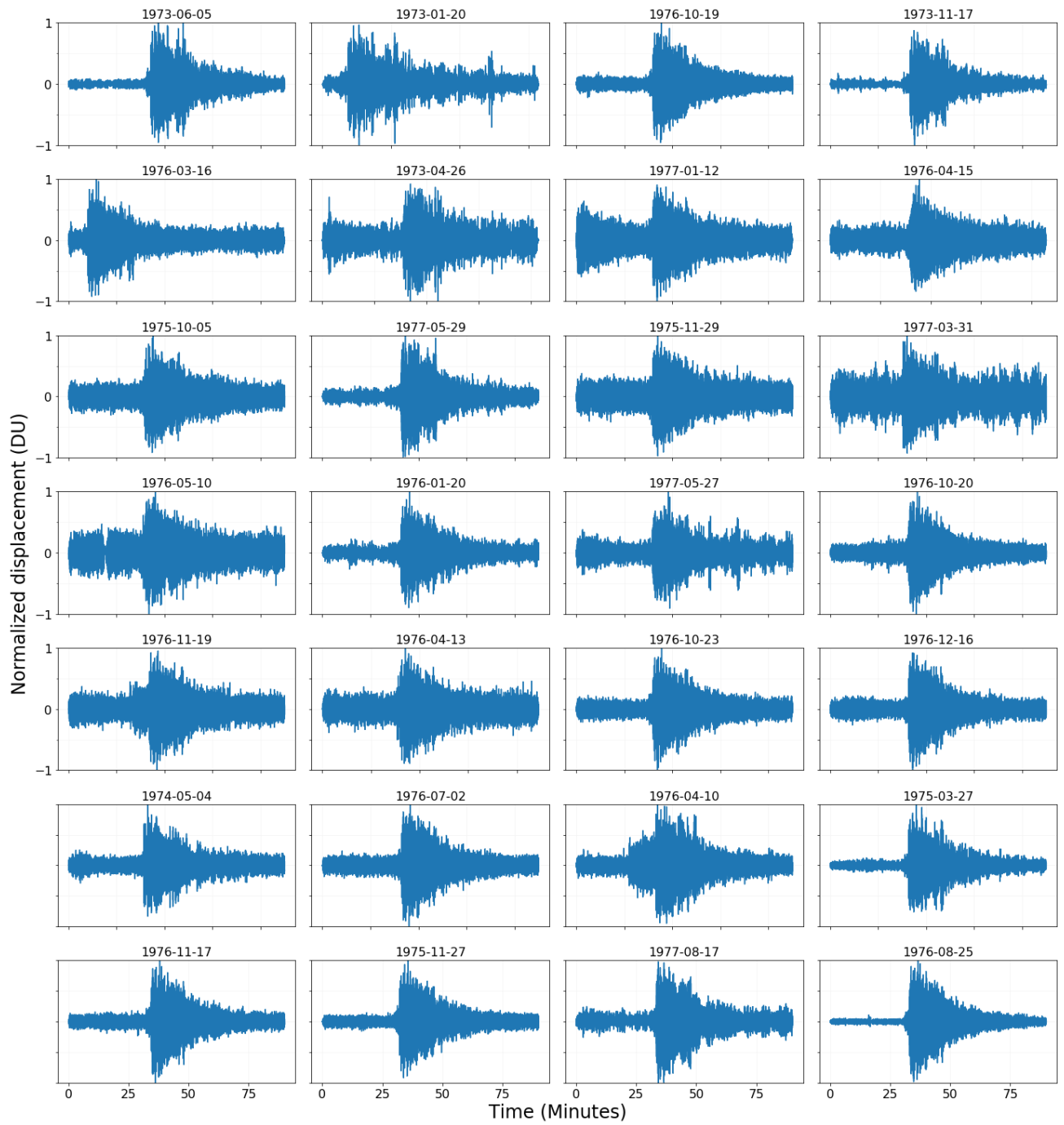
———

April 29, 2022, 4:36pm

Figure S1. Deep moonquake waveforms used for PCA decomposition, recorded at station S12, channel MHE, in the peaked operation mode.
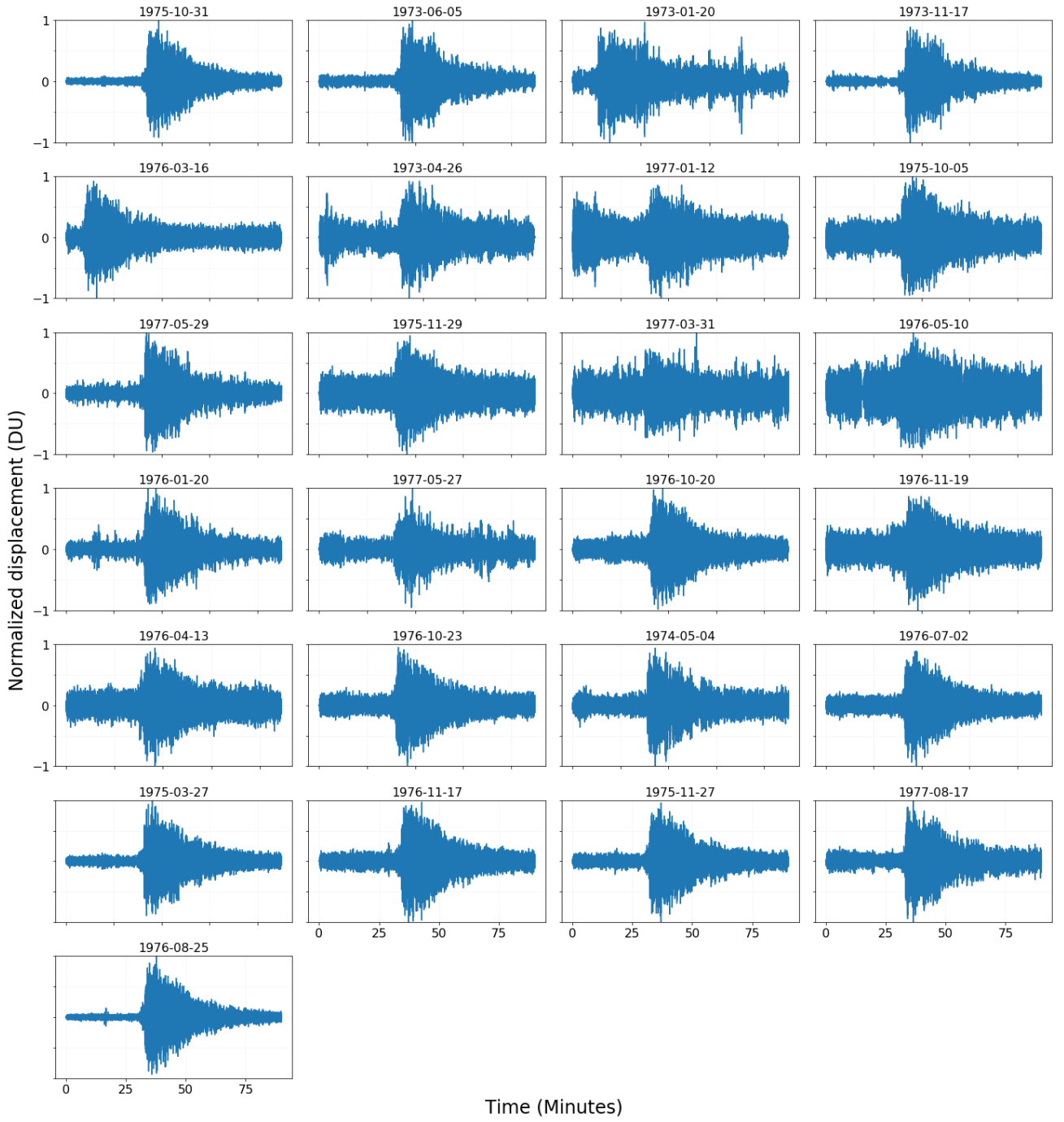
Figure S2. Deep moonquake waveforms used for PCA decomposition, recorded at station S12, channel MHN, in the flat operation mode.
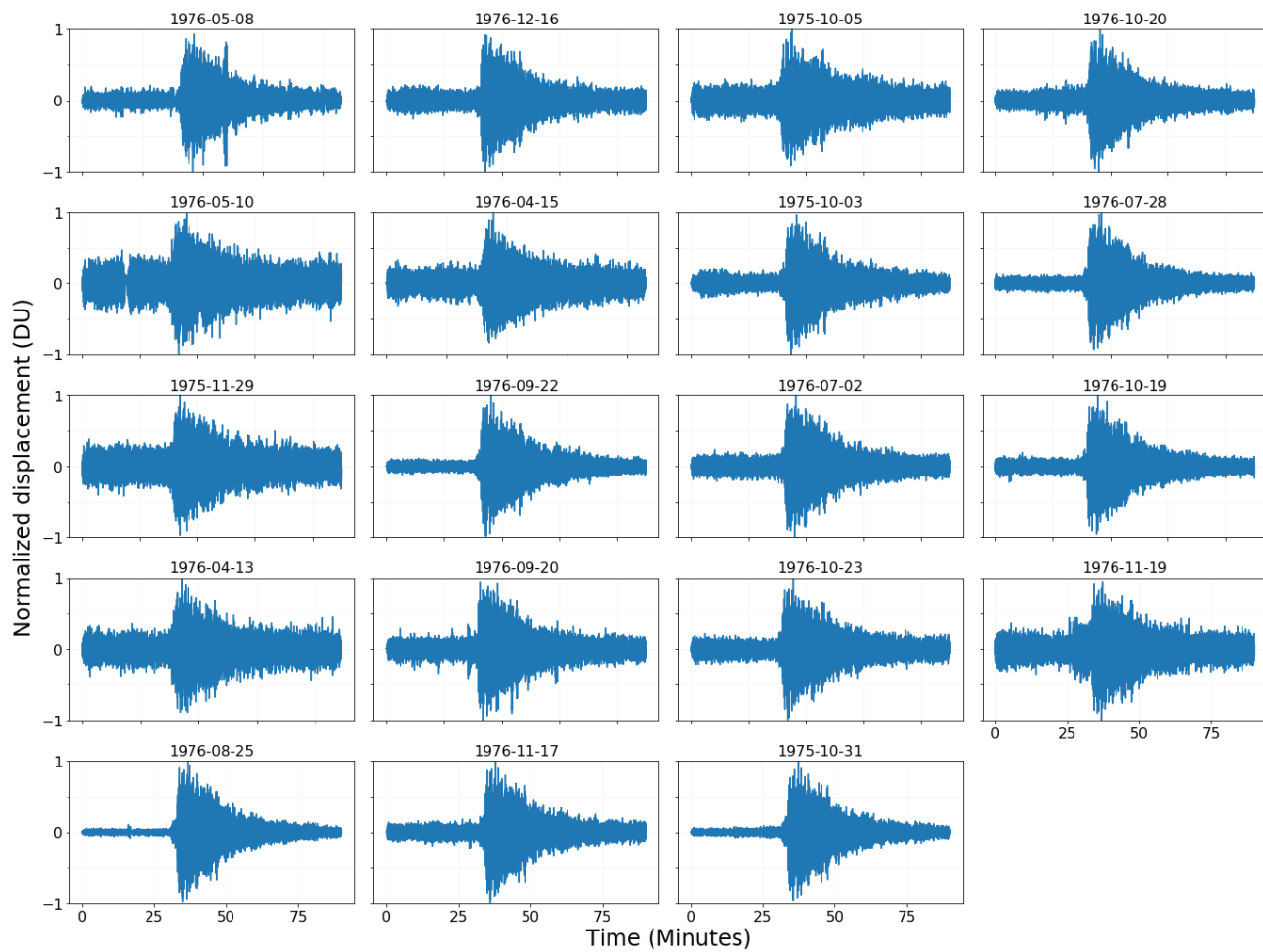
Figure S3. Deep moonquake waveforms used for PCA decomposition, recorded at station S12, channel MHE, in the flat operation mode.

Figure S4. Deep moonquake waveforms used for PCA decomposition, recorded at station S16, channel MHN, in the peaked operation mode.
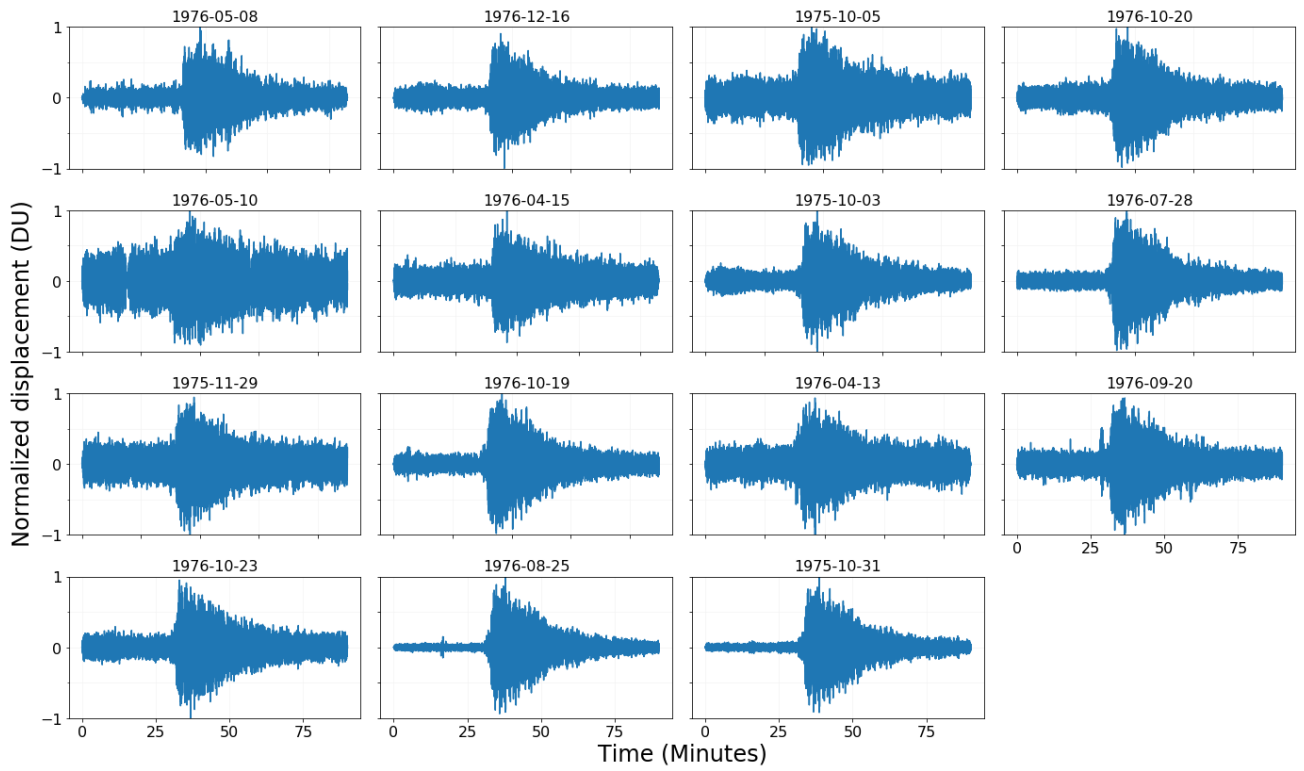
April 29, 2022, 4:36pm

Figure S5. Deep moonquake waveforms used for PCA decomposition, recorded at station S16, channel MHE, in the peaked operation mode.

Figure S6. Deep moonquake waveforms used for PCA decomposition, recorded at station S16, channel MHN, in the flat operation mode.
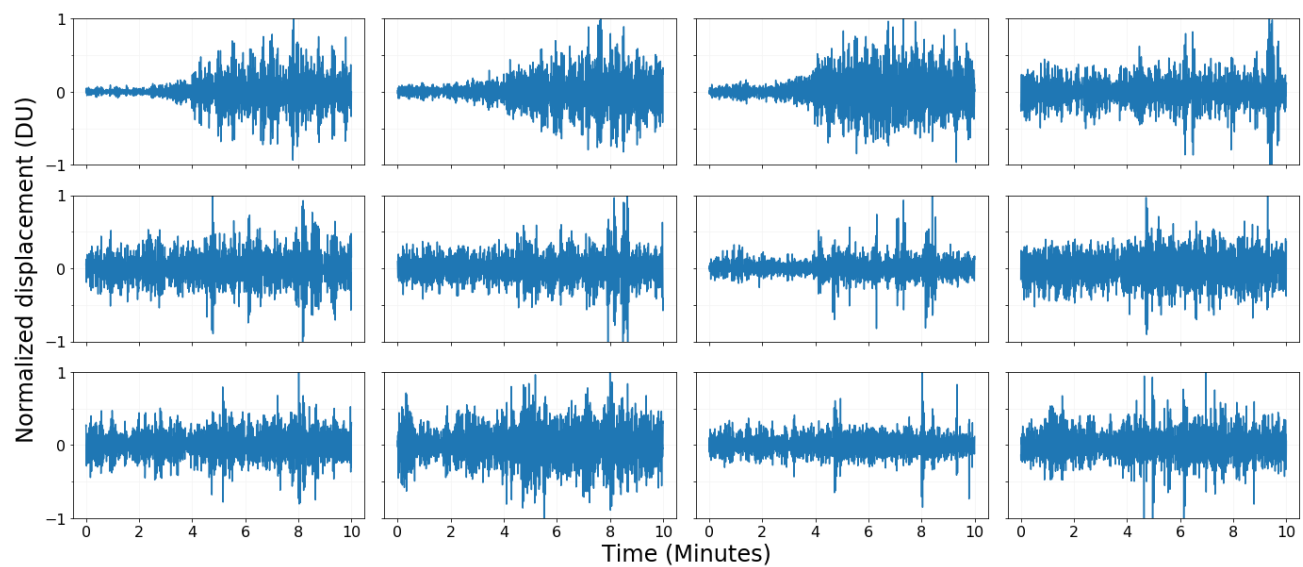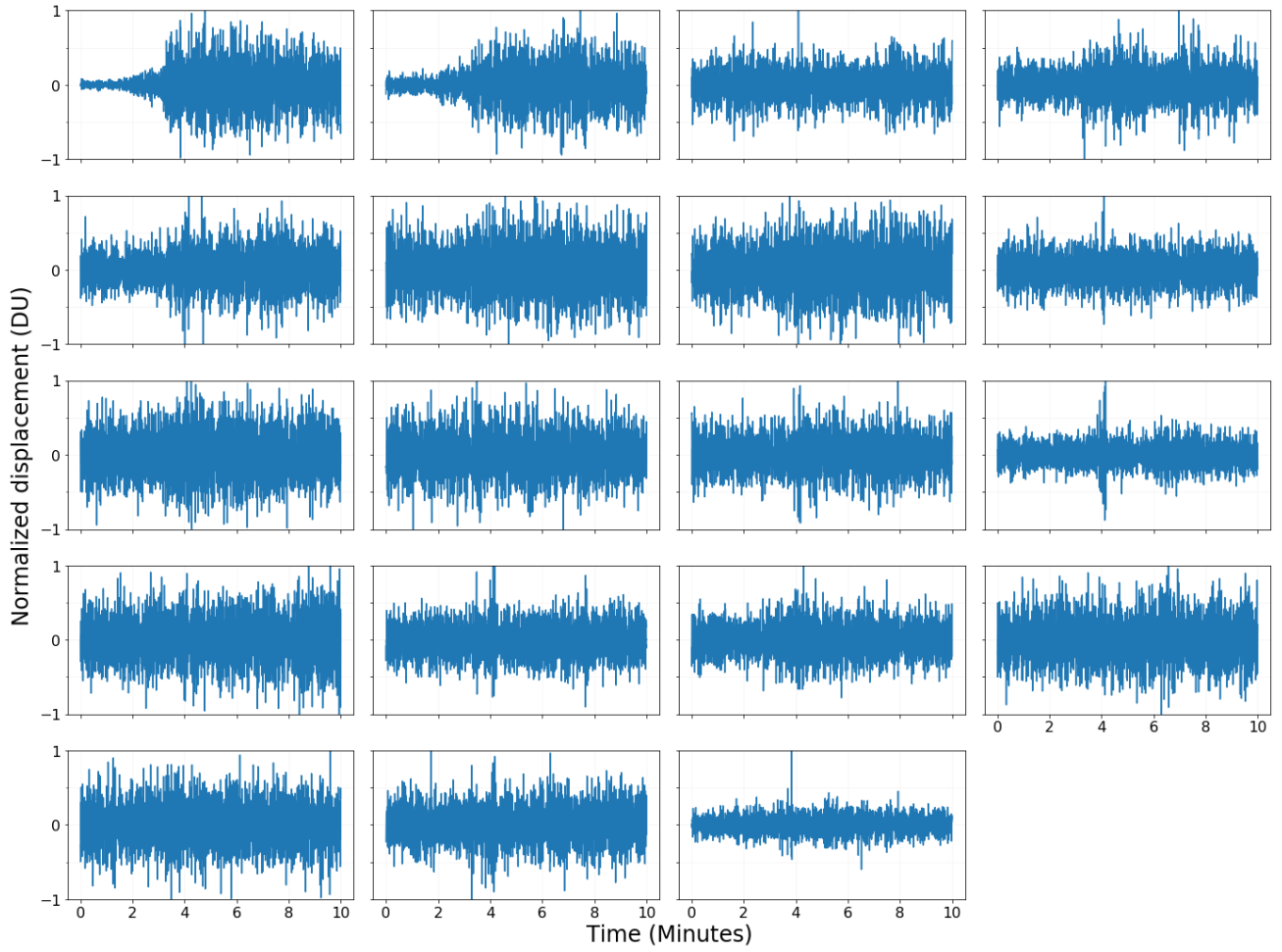
April 29, 2022, 4:36pm

Figure S7.   Deep moonquake waveforms used for PCA decomposition, recorded at station S16, channel MHE, in the flat operation mode.

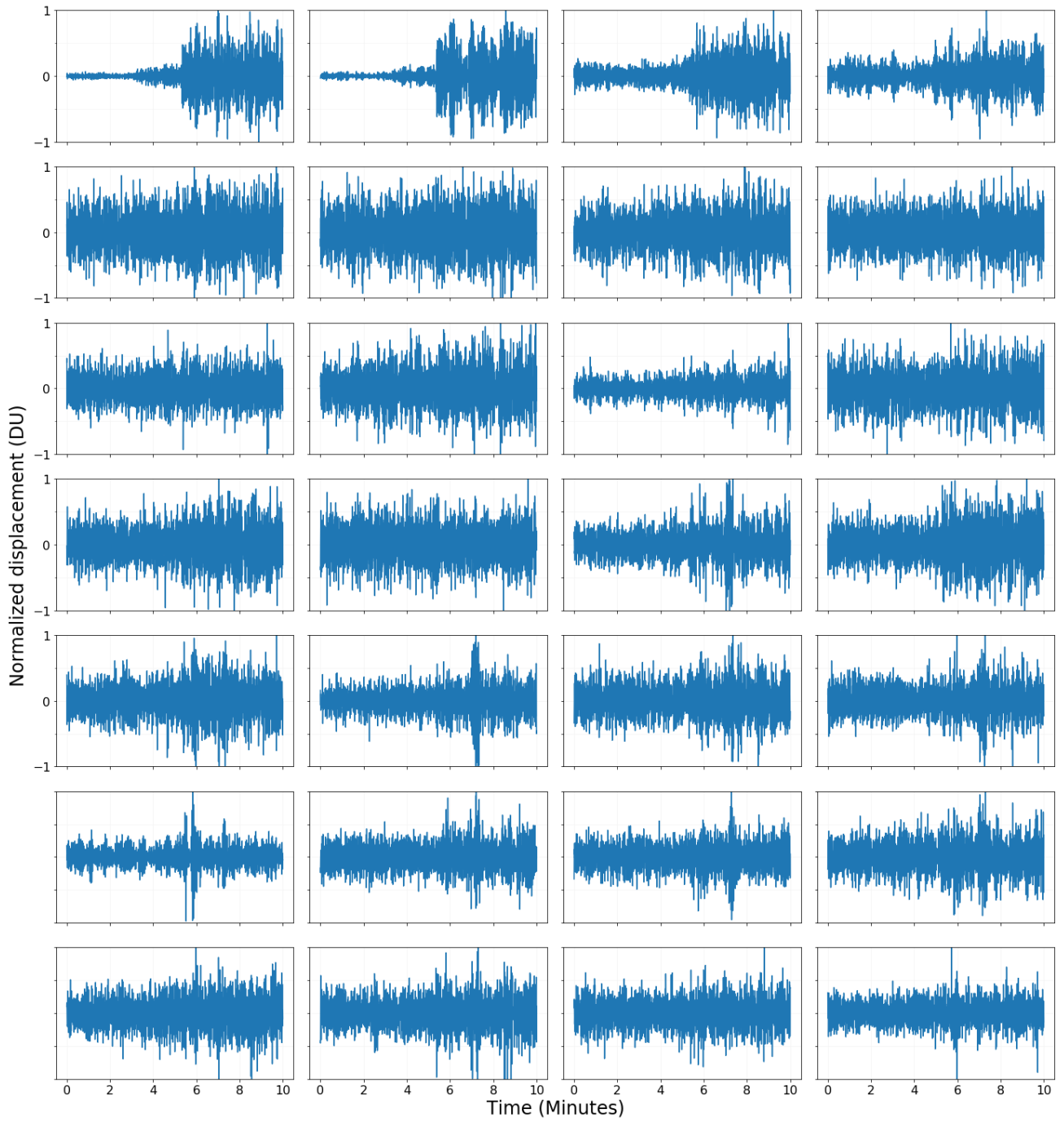**Figure S8.** Principal components derived from the S12 MHE data in the peaked operational mode of the instrument.
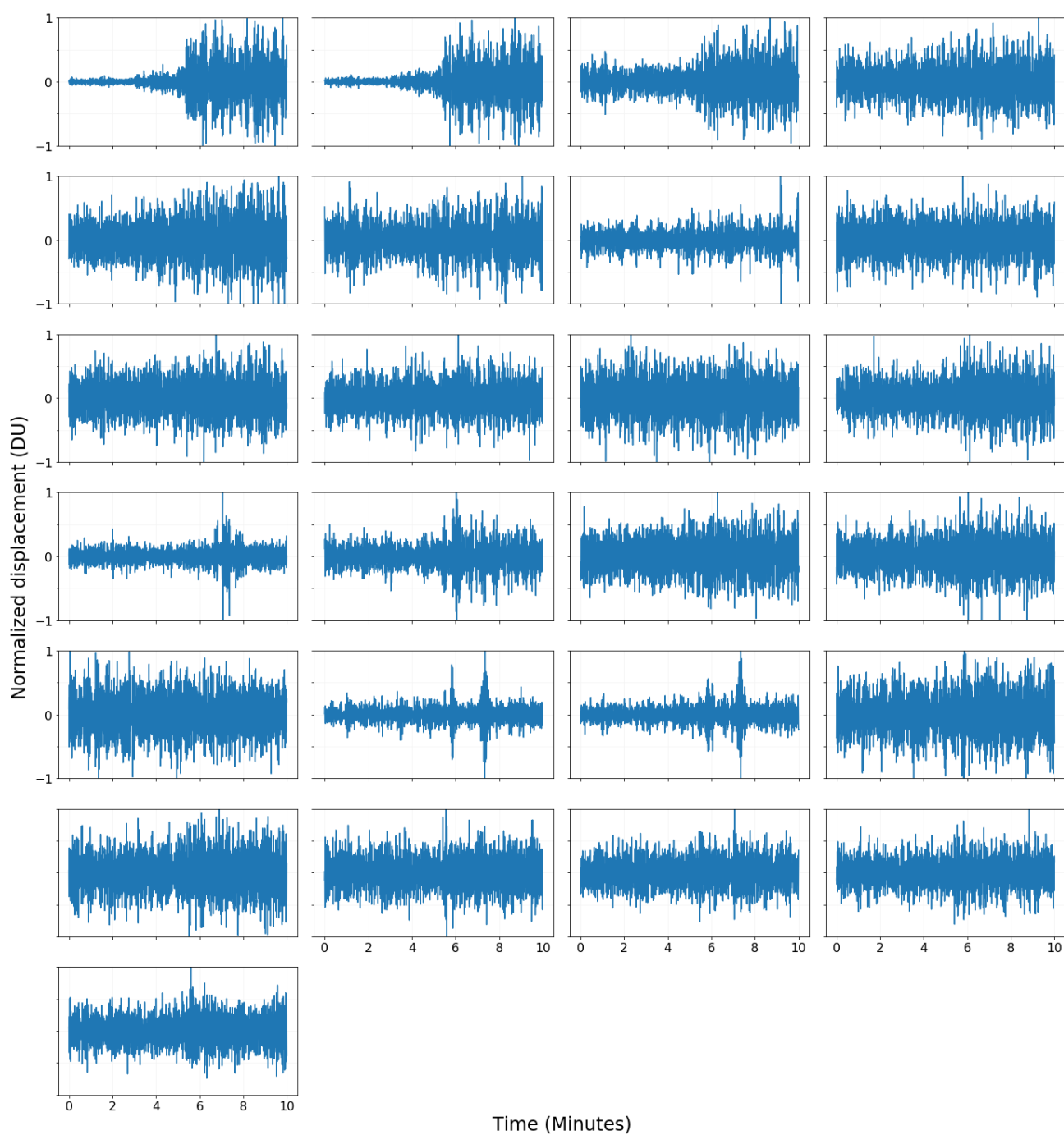
April 29, 2022, 4:36pm

Figure S9. Principal components derived from the S12 MHN data in the flat operational mode of the instrument.
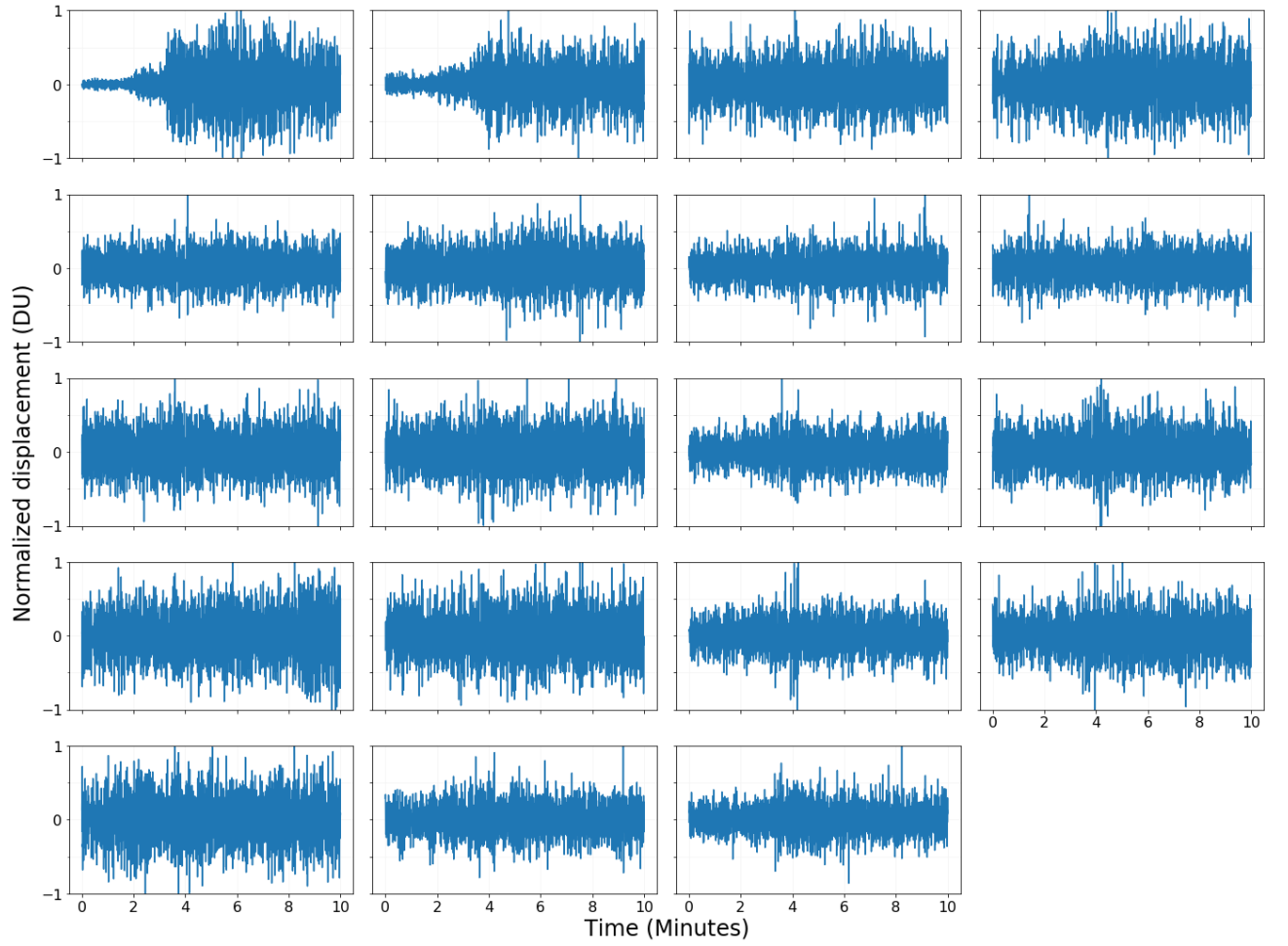
Figure S10. Principal components derived from the S12 MHE data in the flat operational mode of the instrument.
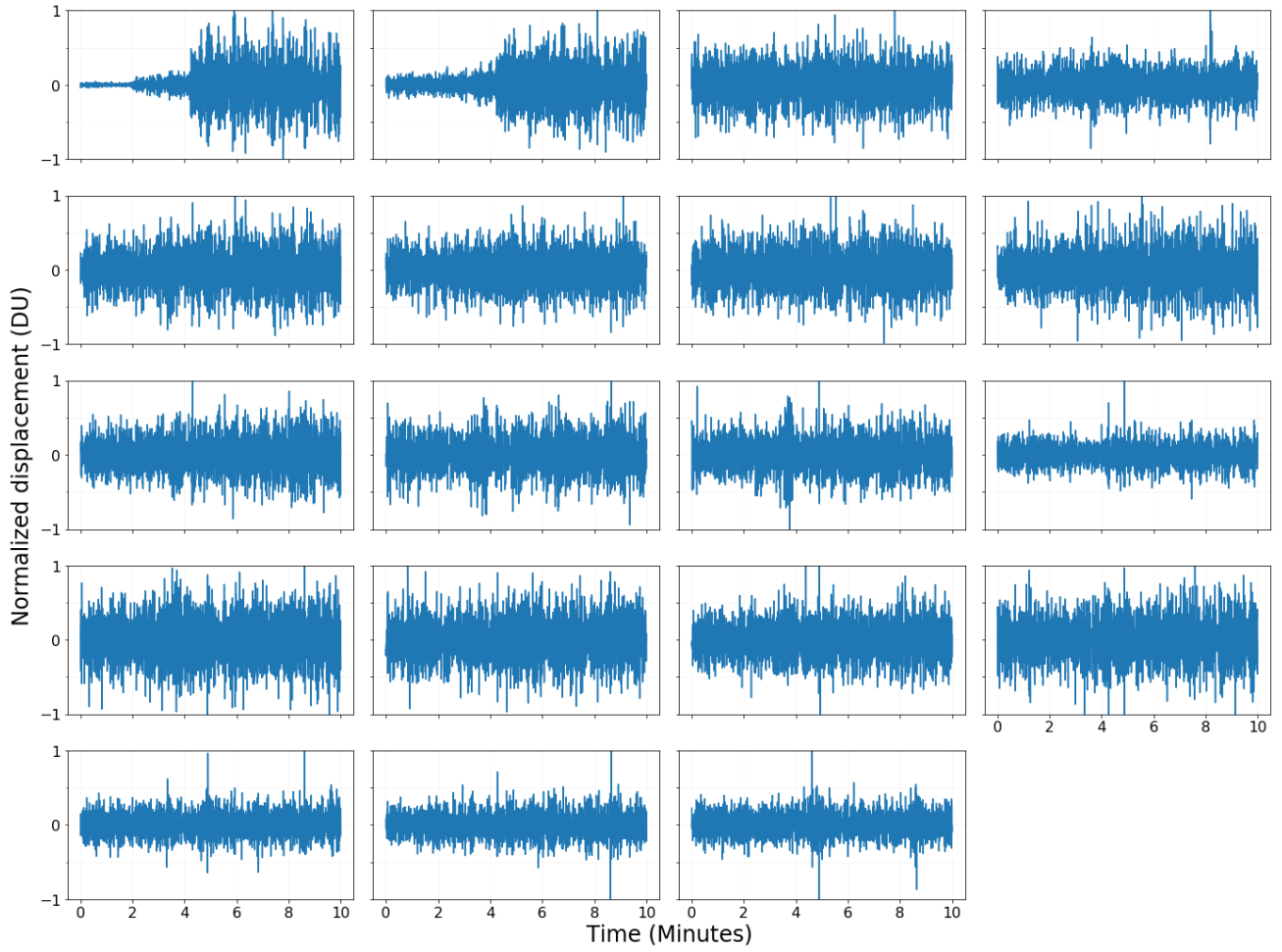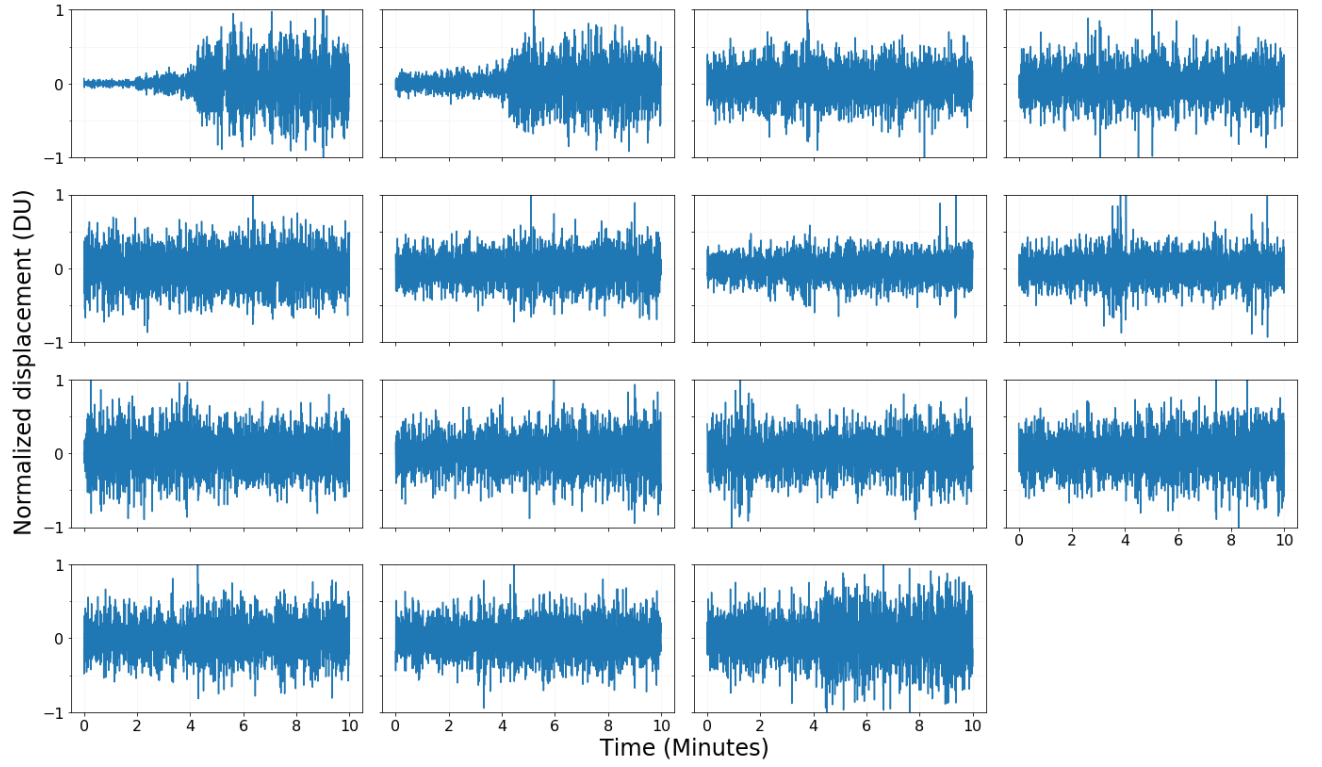
April 29, 2022, 4:36pm

Figure S11. Principal components derived from the S16 MHN data in the peaked operational mode of the instrument.

Figure S12. Principal components derived from the S16 MHE data in the peaked operational mode of the instrument.

Figure S13. Principal components derived from the S16 MHN data in the flat operational mode of the instrument.

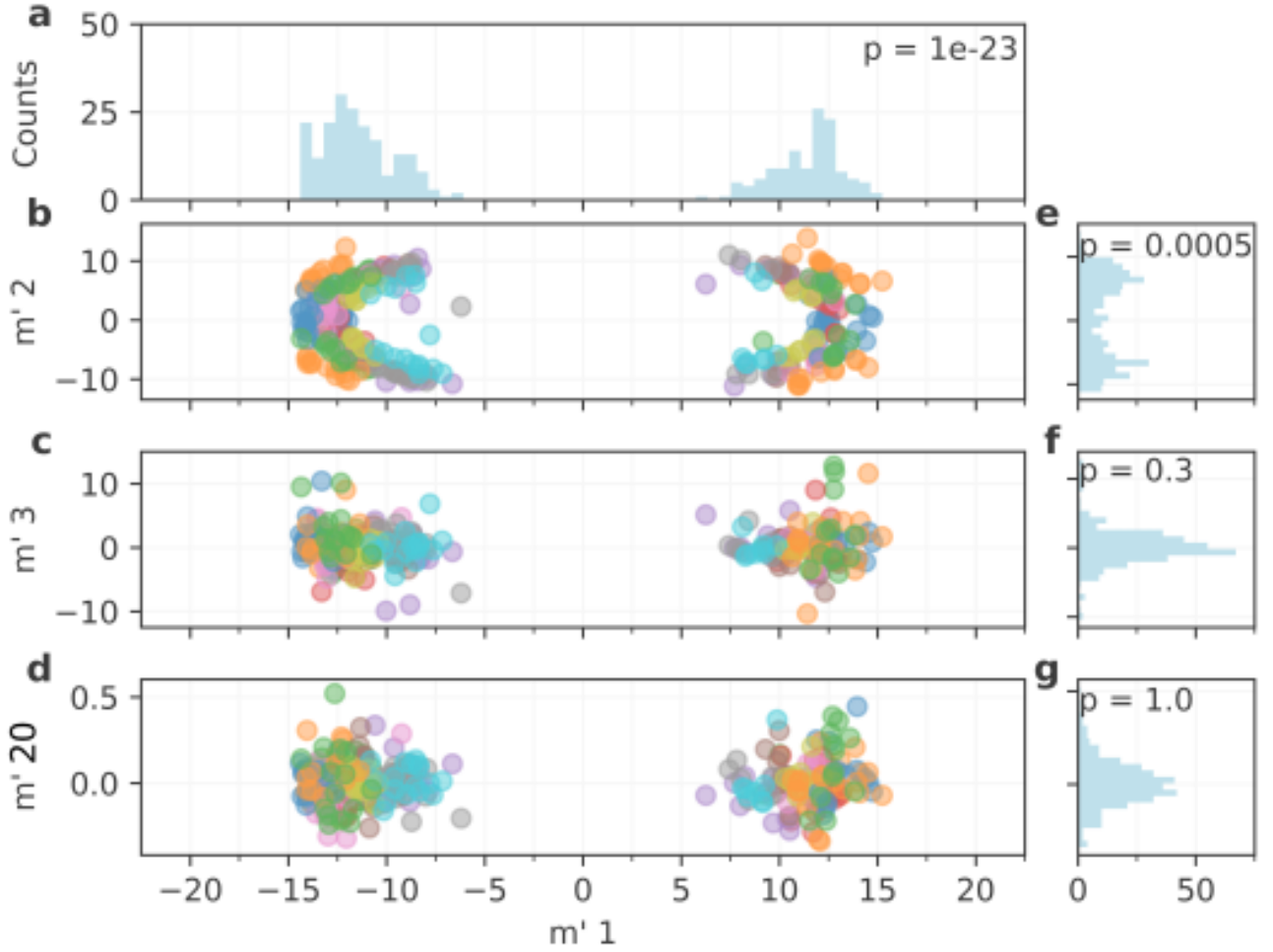**Figure S14.** Principal components derived from the S16 MHE data in the flat operational mode of the instrument.

Figure S15. Unbiased coefficients of the principal components, from the S12 MHE data in the peaked operational mode. In panels b-d, the coefficient for the first principal component m'_{i1} is plotted on the x-axis. The coefficients of the second (m'_2), third (m'_3) and twentieth (m'_{20}) principal components are plotted on the y axis of panels b,c and d, respectively. Each event is plotted in a different colour. Panels a, e, f, and g summarise the distribution of coefficients for each of the principal components. The text in the top of panels a, e, f, and g is the probability (p-value) that each distribution differs from the distribution of the coefficients derived from noise. Only the first two components differ from noise.
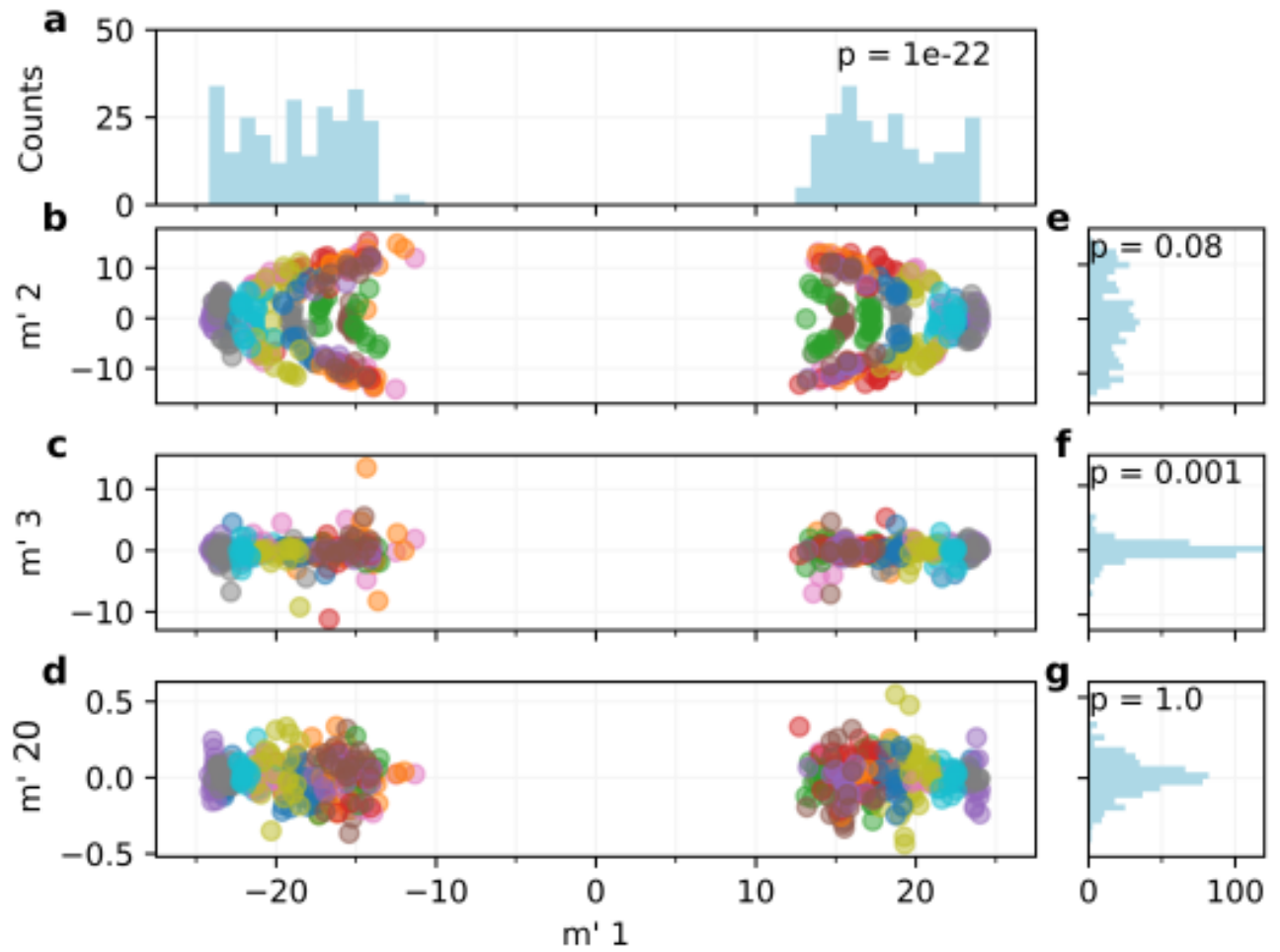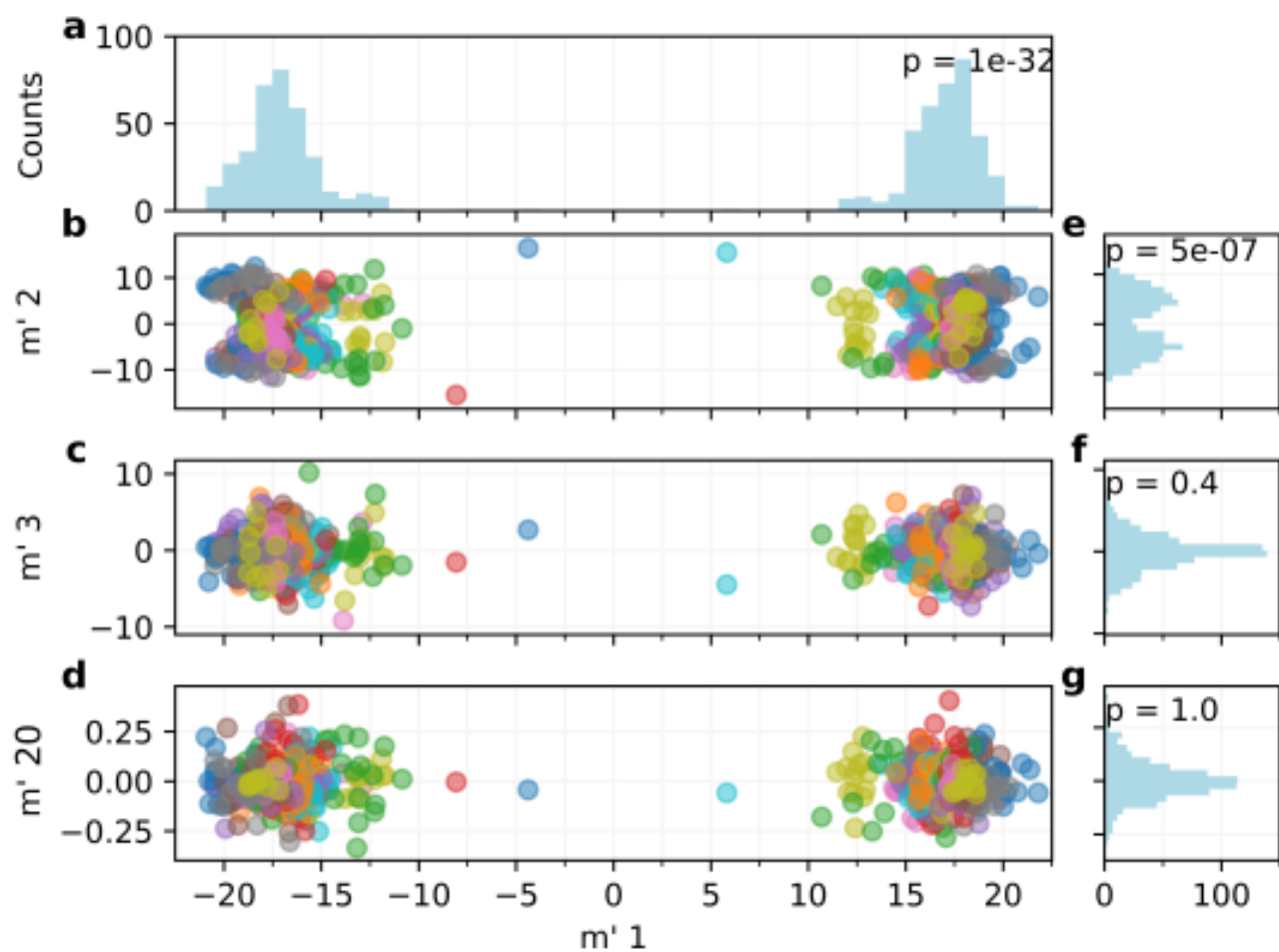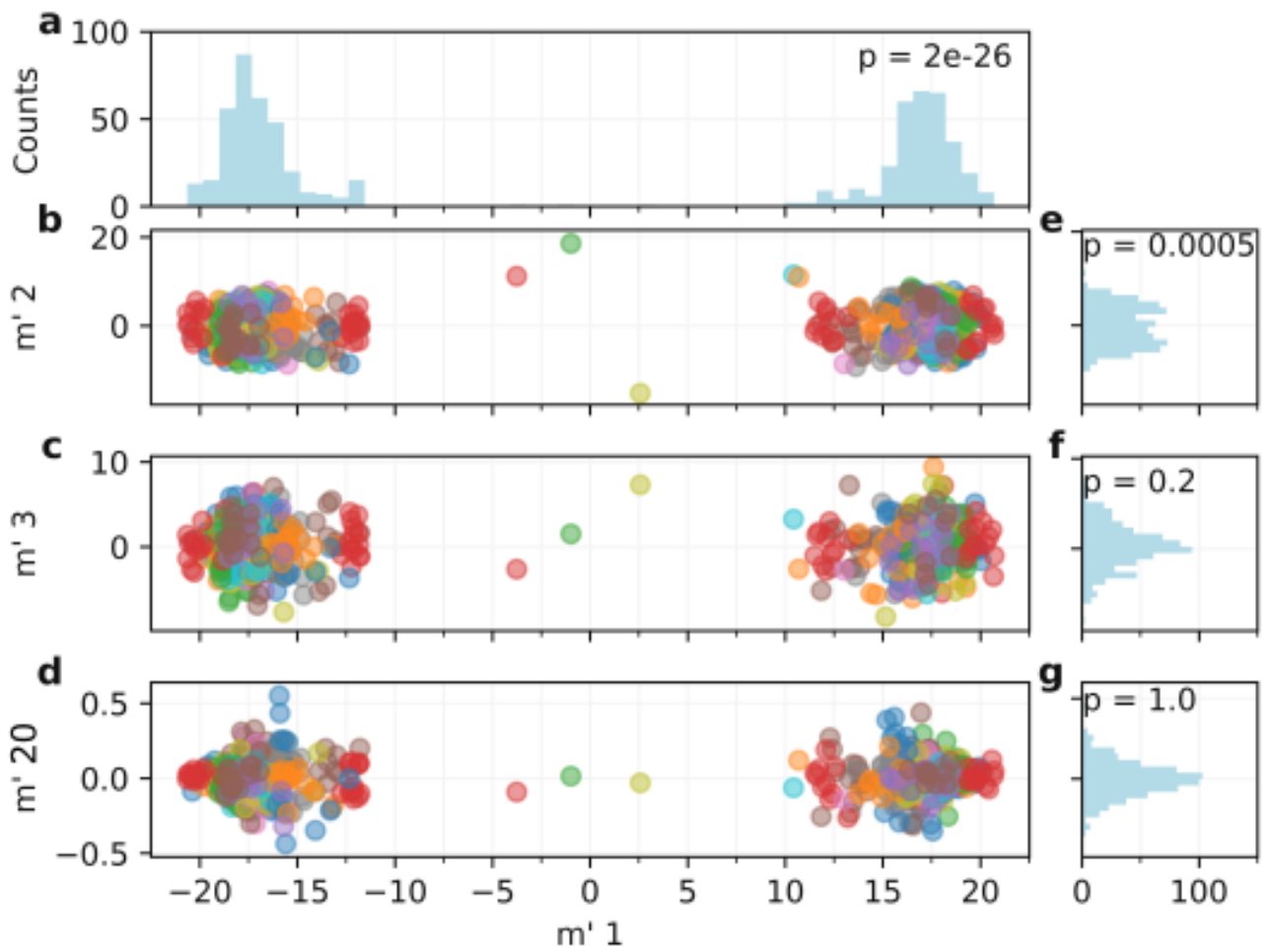
Figure S16. Same as Figure S15 from the S12 MHN data in the flat operational mode.
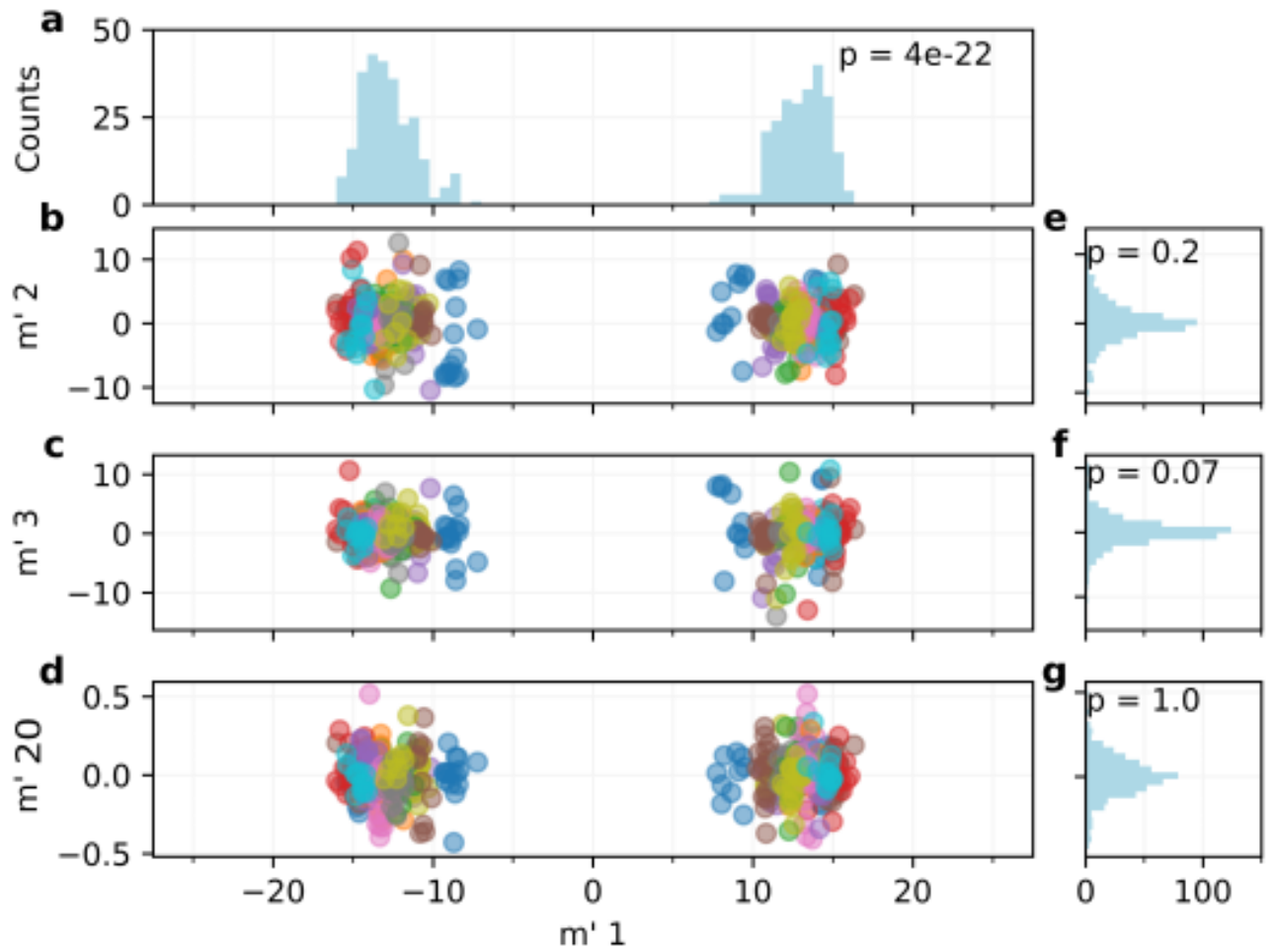
April 29, 2022, 4:36pm
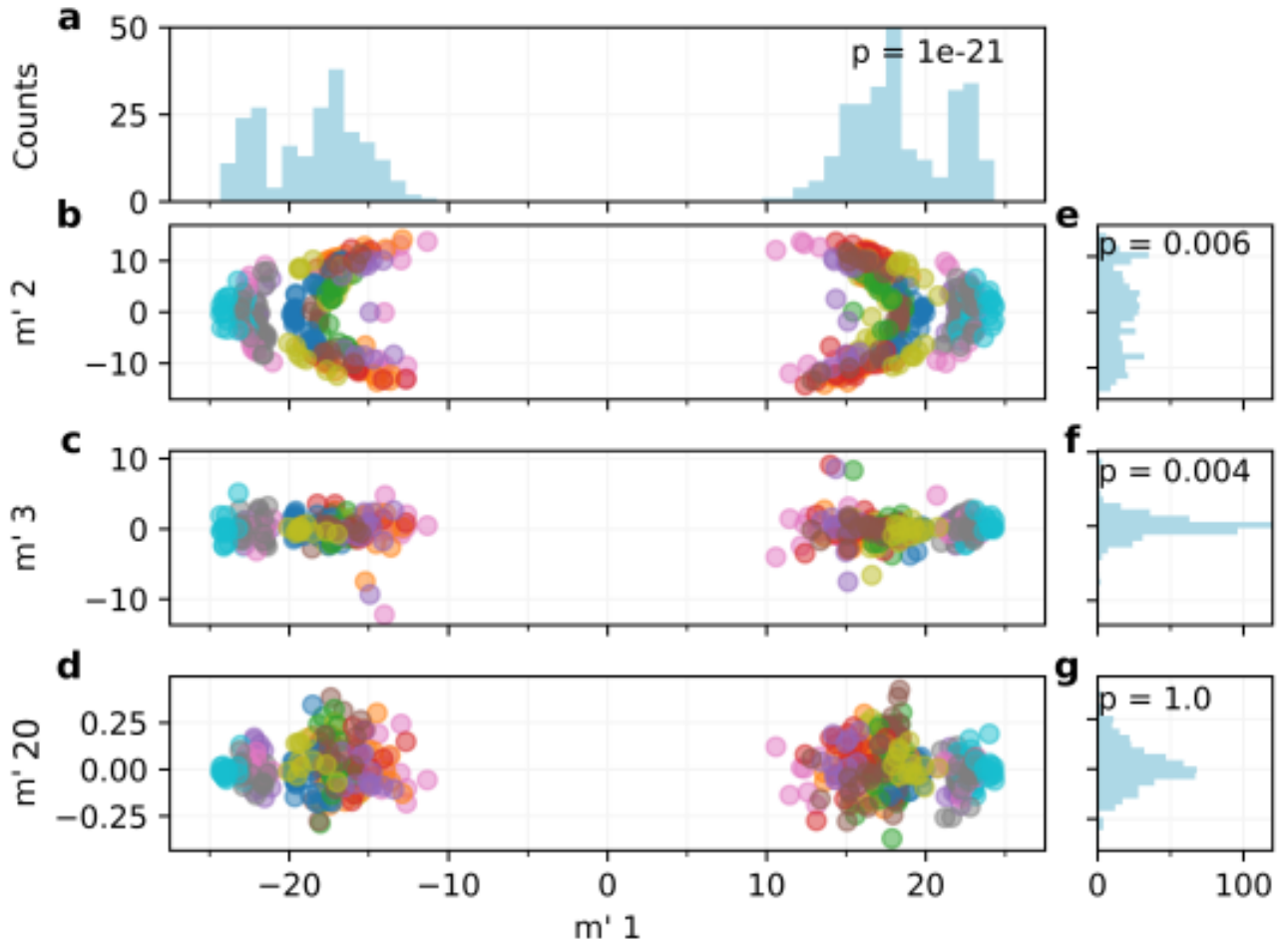
Figure S17. Same as Figure S15 from the S12 MHE data in the flat operational mode.
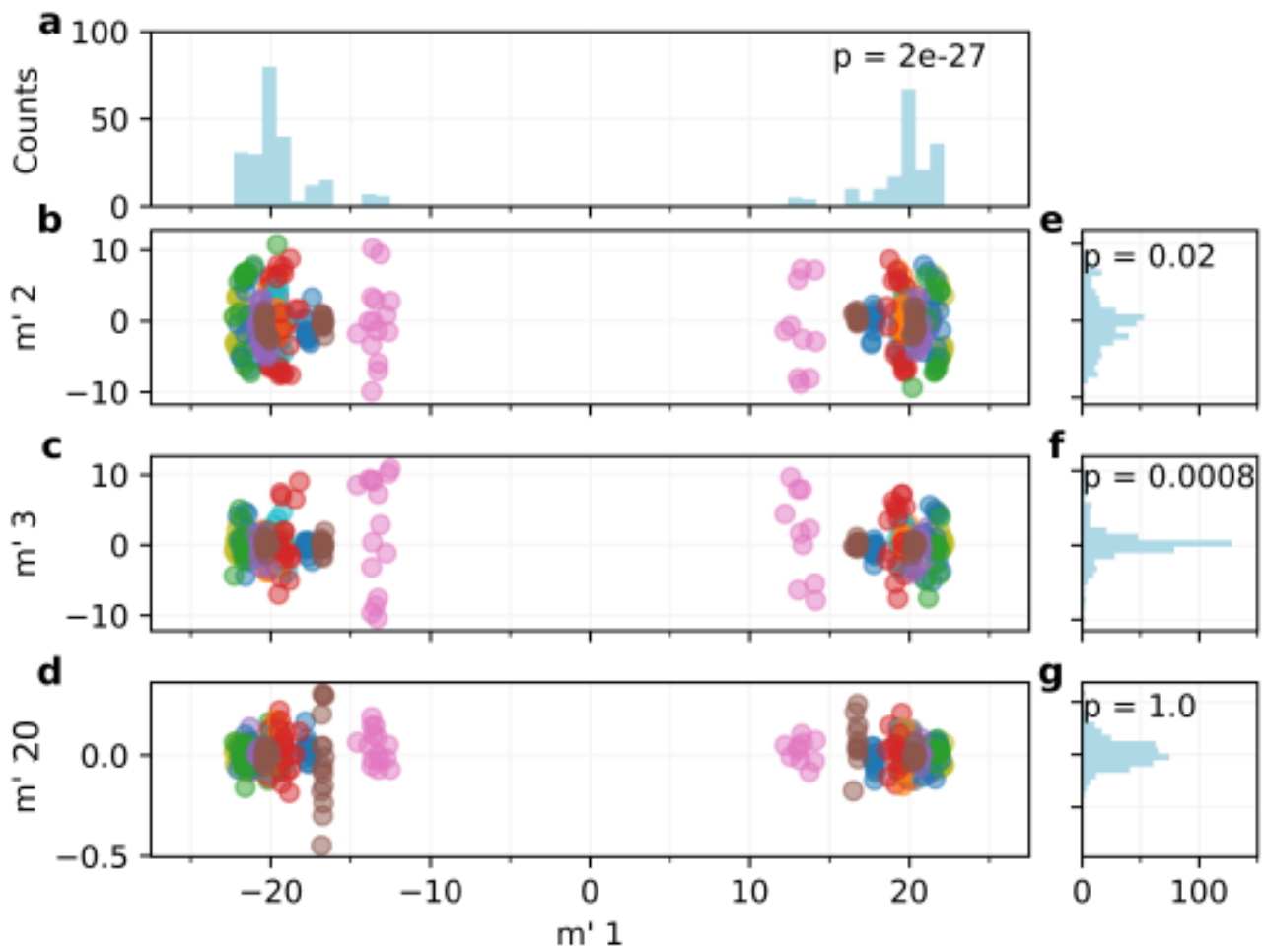
Figure S18. Same as Figure S15 from the S16 MHN data in the peaked operational mode.
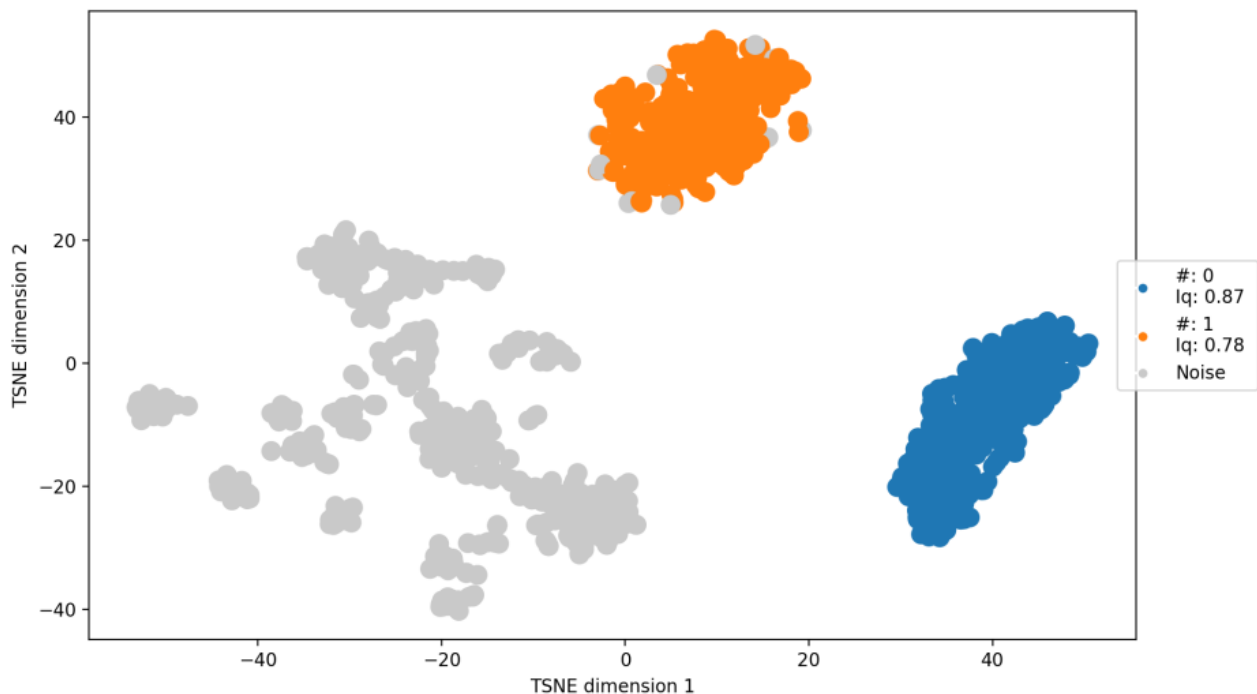
Figure S19. Same as Figure S15 from the S16 MHE data in the peaked operational mode.

Figure S20. Same as Figure S15 from the S16 MHN data in the flat operational mode.

Figure S21. Same as Figure S15 from the S16 MHE data in the flat operational mode.

Figure S22. Clustering results of bootstrapped **G**, obtained for S12 MHE in peaked operational mode. One point is plotted for each bootstrapped estimate of a principal component, but only the first four principal components are plotted. The location of each point is determined by the t-sne algorithm, preserving the similarity of components from the higher dimensional space (Maaten Hinton, 2008; Gaddes et al., 2019). The colour of each point is determined by the HBDSCAN clustering algorithm (McInnes et al., 2017; Gaddes et al., 2019). Grey points represent component estimates that are not assigned to a cluster.
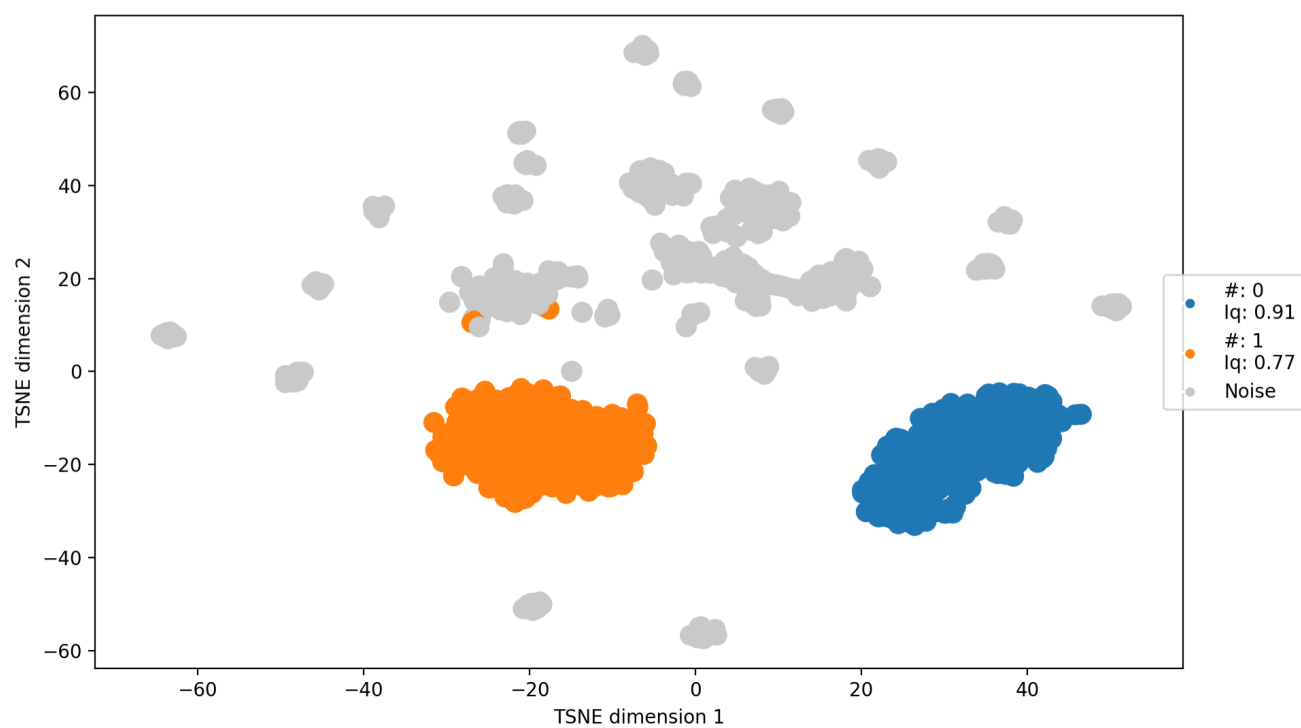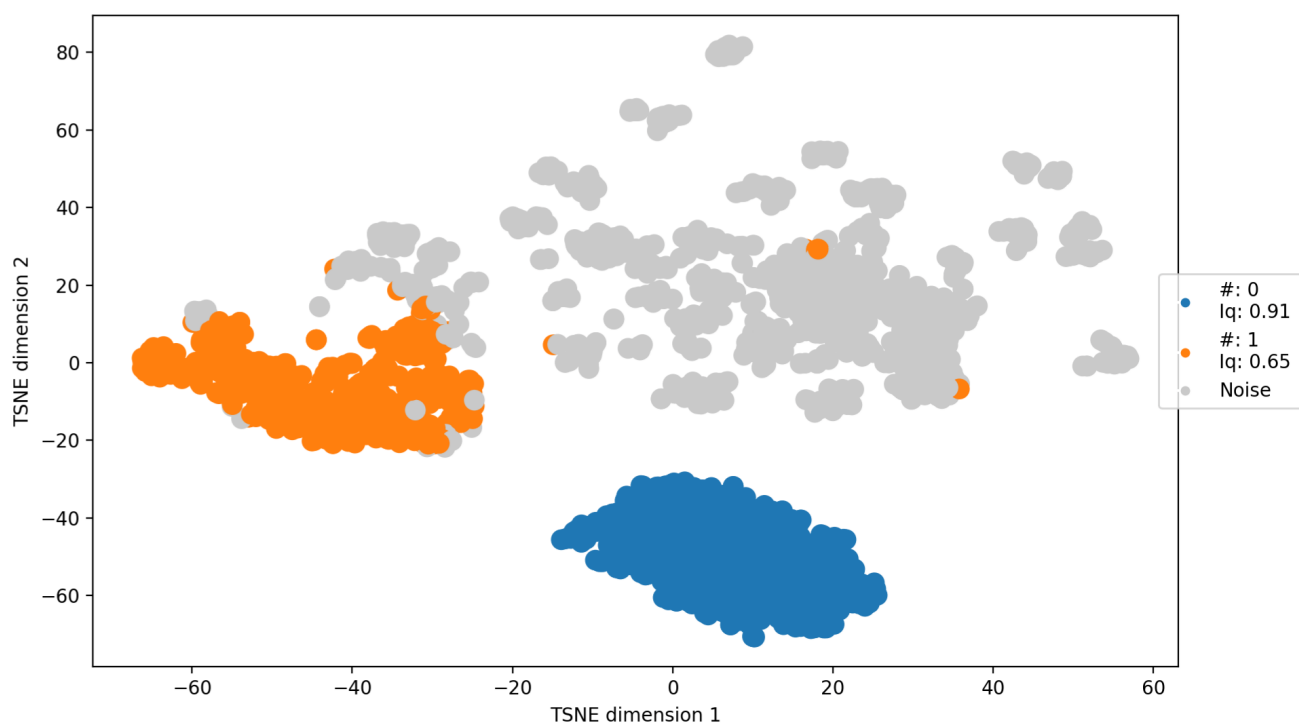
Figure S23. Same as Figure S22 obtained for S12 MHN in flat operational mode.
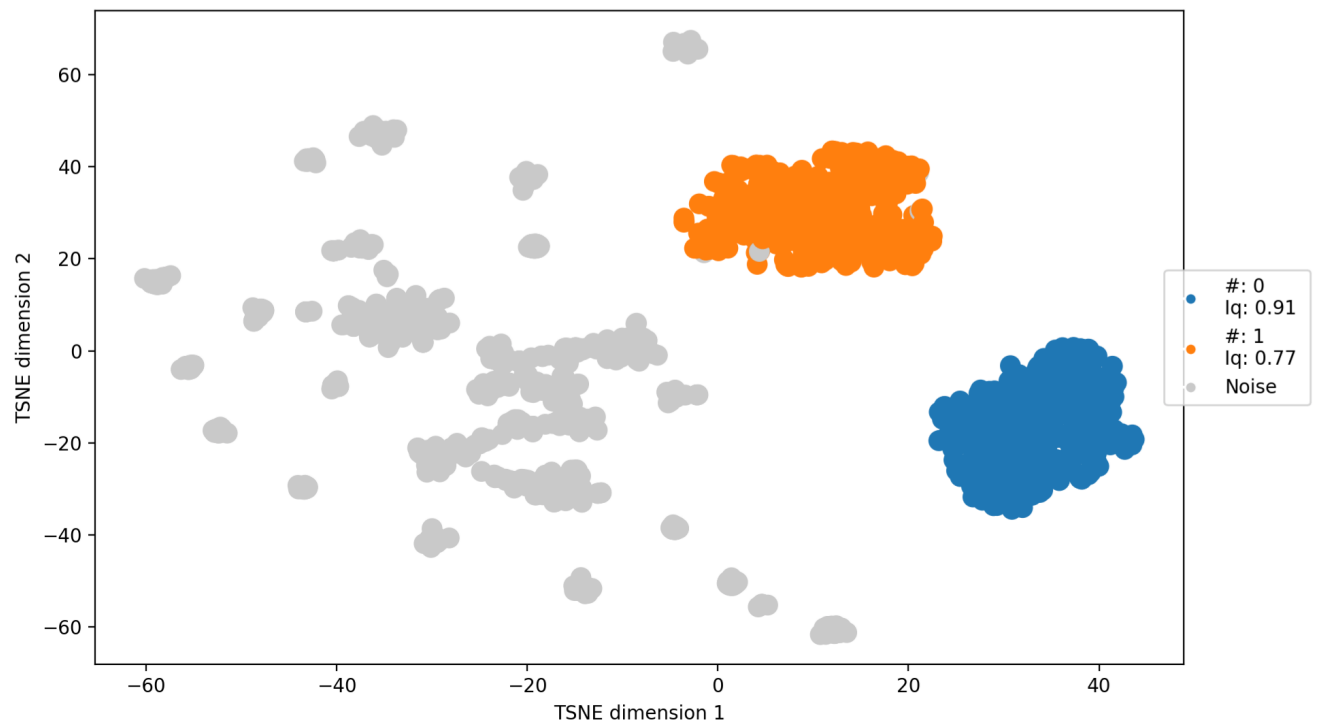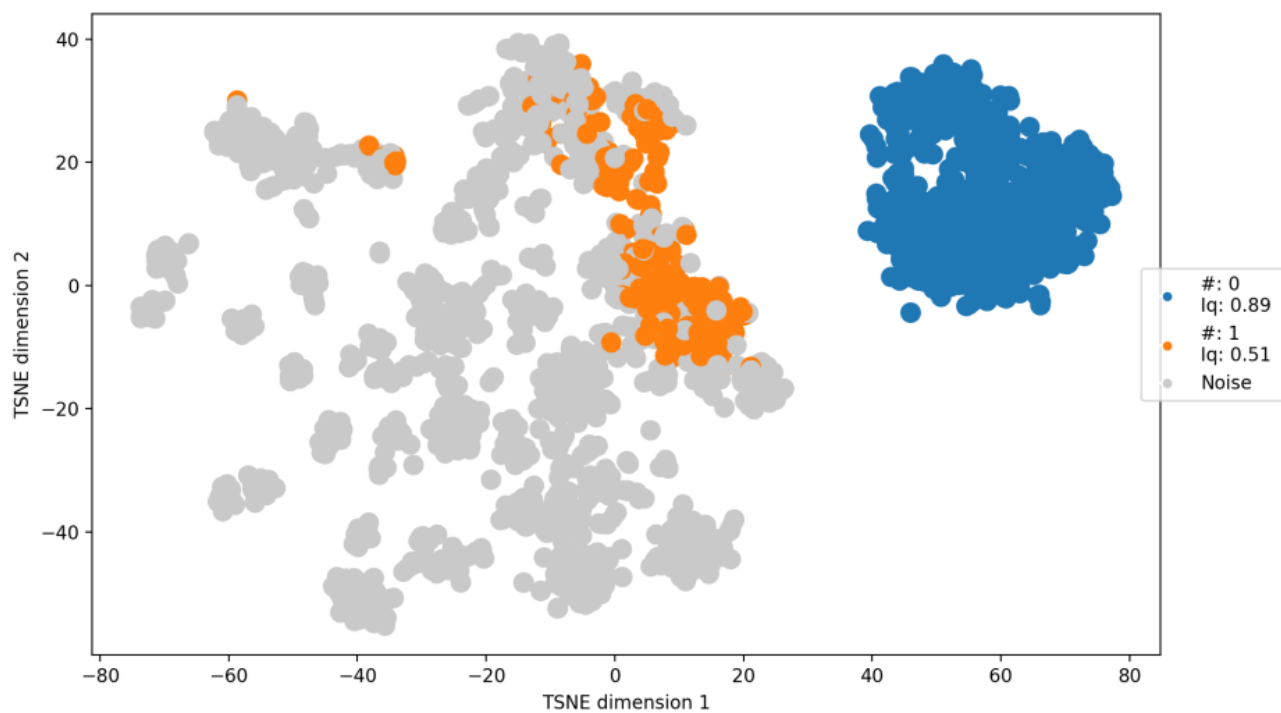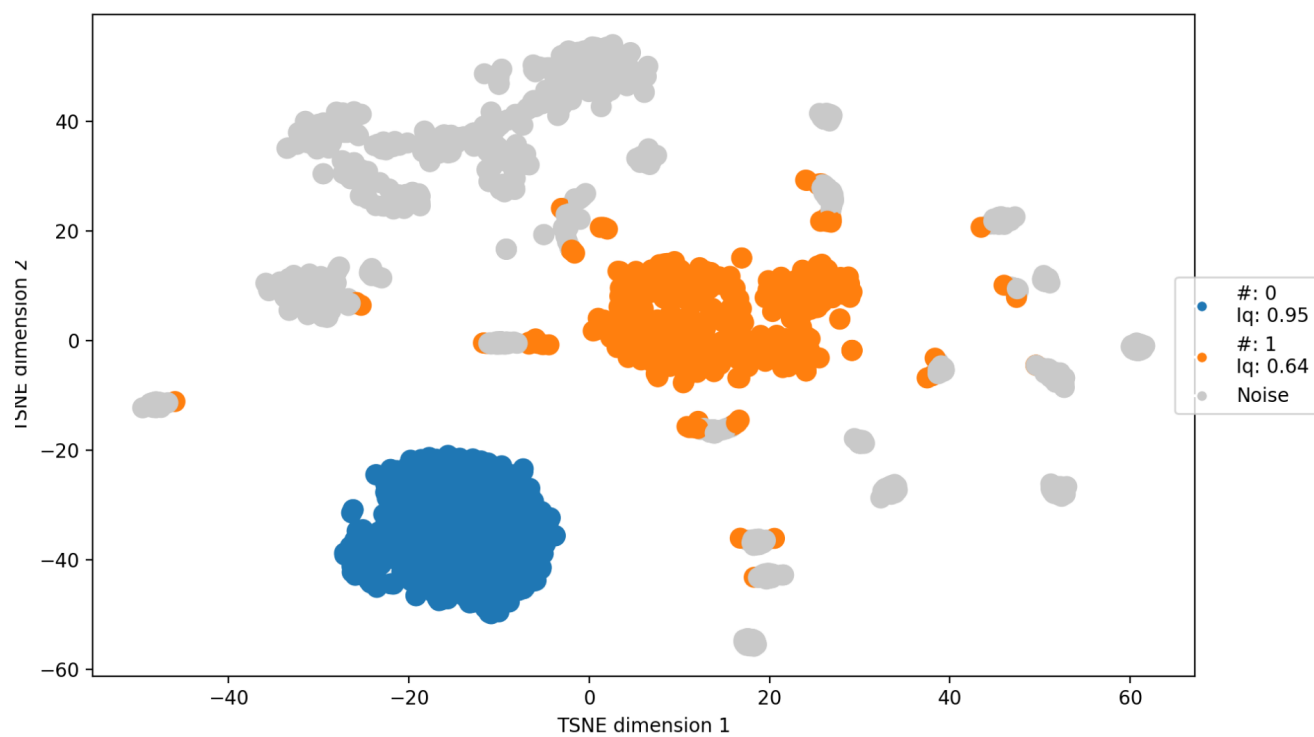
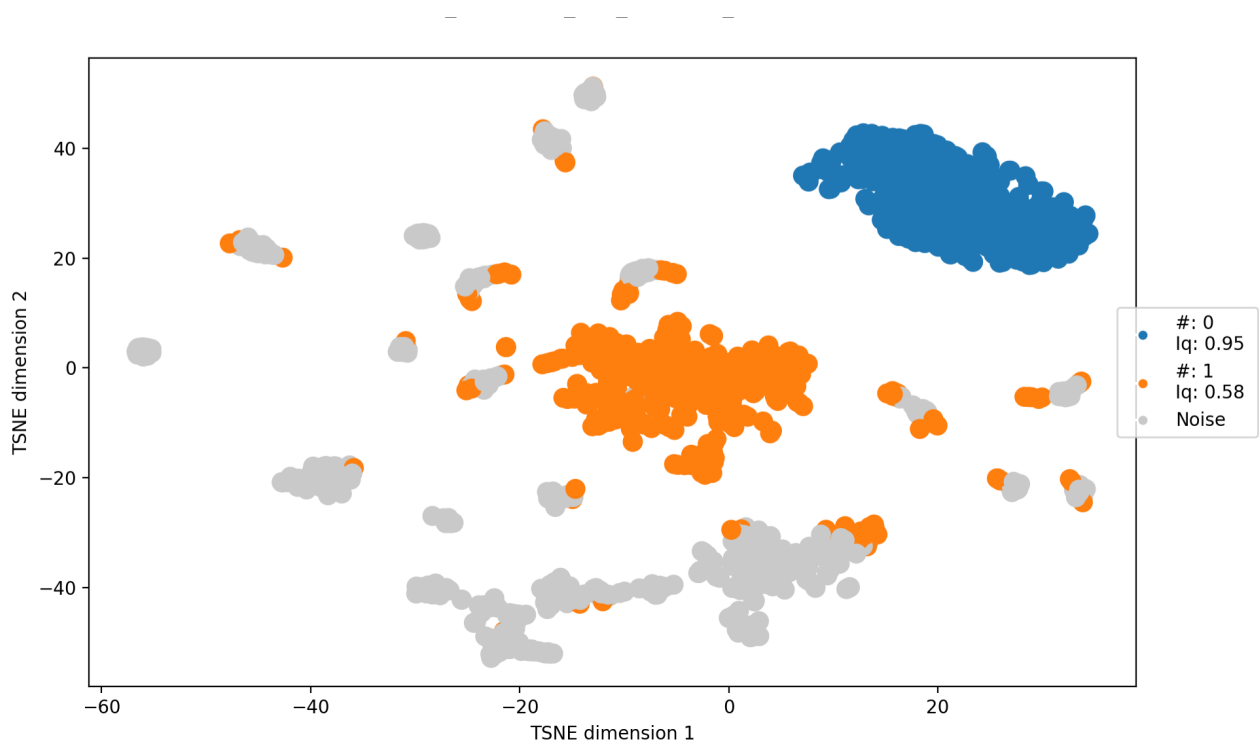**Figure S24.** Same as Figure S22 obtained for S12 MHE in flat operational mode.

Figure S25. Same as Figure S22 obtained for S16 MHN in peaked operational mode.

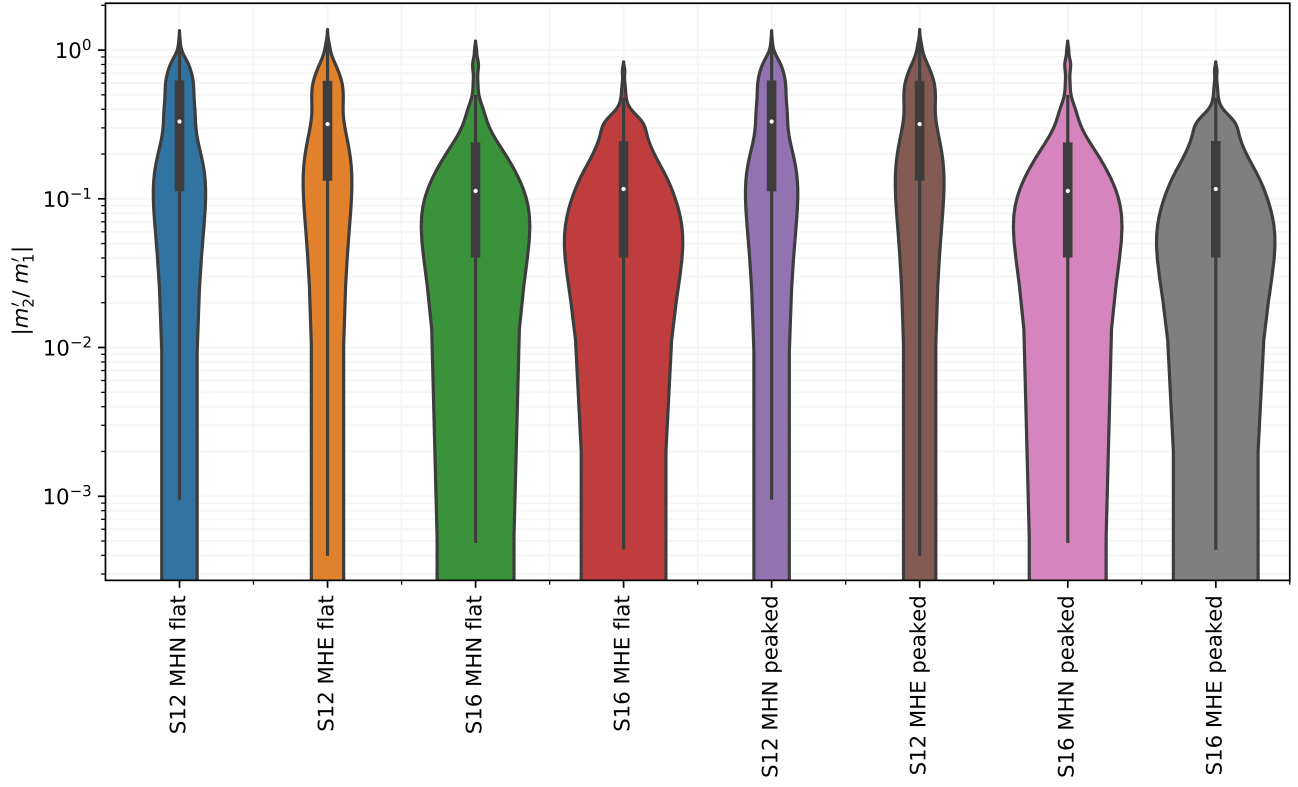**Figure S26.** Same as Figure S22 obtained for S16 MHE in peaked operational mode.

Figure S27. Same as Figure S22 obtained for S16 MHN in flat operational mode.

Figure S28. Same as Figure S22 obtained for S16 MHE in flat operational mode.

Figure S29. Slip coefficient ratio m_2'/m_1' for each station and channel, now plotted with a log axis. The white dot marks the median bootstrapped ratio at each station, the black bar delimits the interquartile range, and the thin black line delimits $1.5 \times$ the inter-quartile range. The coloured areas illustrate the probability density of the ratio at each station.